Proceedings 10th NUMGE 2023
10th European Conference on Numerical Methods in Geotechnical Engineering
Zdravkovic L, Kontoe S, Taborda DMG, Tsiampousi A (eds)

https://doi.org/10.53243/NUMGE2023-184

System for automated design of offshore rock berms

K. Krabbenhøft[1] , J. Krabbenhøft[1] , C. Olsen[2]

[1] *Optum Computational Engineering, Copenhagen, Denmark*
[2] *Subsea7, Stavanger, Norway*

ABSTRACT: A system for automated design of offshore rock berms is described. The main idea is to extract 2D sections on the basis of the actual 3D geometry (seabed topography and berm geometry). These sections are then processed, first with a bespoke Limit Equilibrium procedure and next via Finite Element Limit Analysis. The end result is a rapid method for automated design of offshore rock berms. In the present paper the seabed is a soft clay, but the methodology is in principle applicable to any material whose strength characteristics is described reasonably with the standard Mohr-Coulomb failure criterion.

Keywords: Finite element limit analysis, limit equilibrium, stability analysis, rock berms, offshore geotechnics.

1 INTRODUCTION

Iceberg plough marks from the last glacial period are a common feature of the seabed of the Norwegian Sea. The plough marks are in the form of long canyons some 2 to 10 m deep. An example is shown in Figure 1. Ice berg plough marks are a substantial challenge in the design of offshore pipelines. In particular, the question is whether the pipe line will be able to span a given plough mark freely within suffering excessive strains. If not, intervention in the form of a rock berm is necessary. Rock berms are embankment type structures constructed on the seabed on which the pipe line is supported to traverse the plough mark. The total volume of typical rock berms may range from a few hundred to tens of thousands of cubic metres. An example of a rock berm traversing a plough mark is shown in Figure 2.

The design of offshore rock berms is complicated by the fact that the seabed sediments often are very soft, typically with an undrained shear strength of a 1-2 kPa at the surface and increasing 1-2 kPa/m with depth. This often renders berms such as the one shown in Figure 2 unstable. To stabilize a given berm, so-called counterfill may be added. These are additional berm-type structures extending out from the main berm. An example is shown in Figure 3.

The design of rock berms thus comprises an iterative sequence of stability analyses with modification of the counterfill in each iteration to obtain the smallest possible final volume.

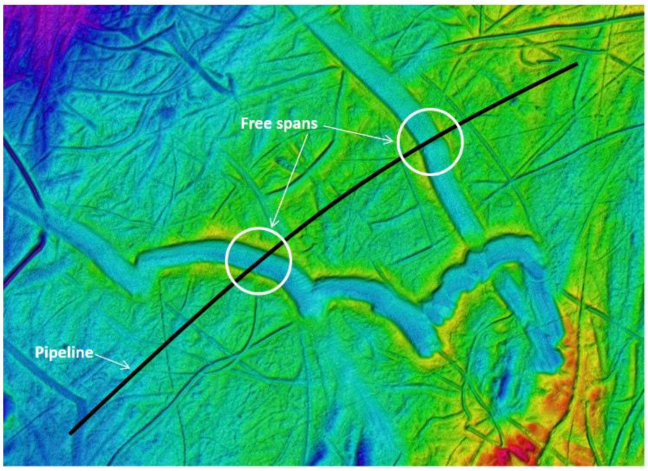

Figure 1. Pipeline on seabed with plough marks (red is 240 m water depth, purple is 248 m).

Although rock berms are obvious 3D structures, their design has traditionally been carried out by considering an appropriate selection of 2D sections. This approach is conservative (provided the critical sections are identified), but has advantages in terms of computational requirements, leading, generally speaking, to less total design time.

Also traditionally, rock berm design has been carried out in a manual, sequential manner with each rock berm along a given route being designed by first extracting a number of sections and then iteratively modifying the counterfill to ensure overall stability (Eiksund et al. 2008).

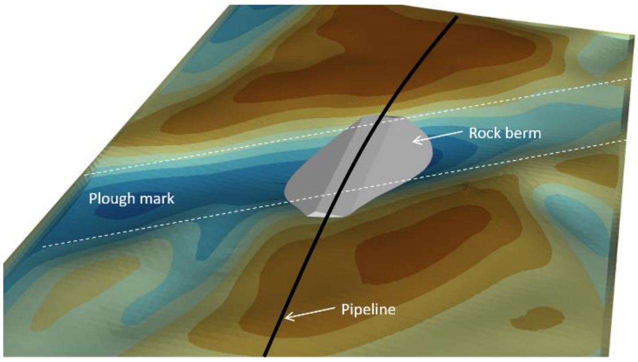

Figure 2. Rock berm (volume ≈4,000 m³).

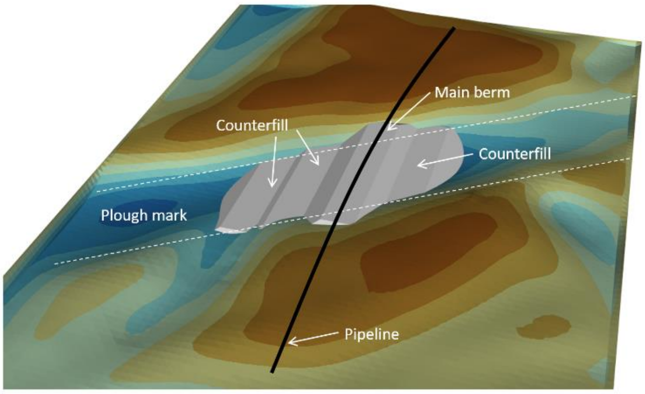

Figure 3. Rock berm with counterfill.

A typical berm requires consideration of some 10-20 sections. Assuming that 10 iterations are required to obtain a satisfactory design, some 100-200 2D stability analyses are required. Assuming further that a given pipeline route comprises some 50-100 berms, the total number of analyses is of order 5,000-20,000. Assuming 1 min of computational time per analysis puts the total computational time in the range of a few days to a few weeks. This time, however, would typically be eclipsed by the time required for setting up models, decision making in each design iteration, etc. As such, in the best case, the design of a complete pipeline route easily takes several months. Finally, if changes are made to the pipeline route, the entire process needs to be repeated.

In the following, a strategy for automated design of rock berms is described. The strategy is roughly equivalent to the manual one. First, relevant 2D sections are extracted based on an analysis of the topography. A typical section is shown in Figure 4. Stability analyses for each section are then conducted using a bespoke Limit Equilibrium (LE) procedure. Then, on the basis of the results, a decision is made with respect to counterfill. The entire cycle is then repeated until all sections are stable. Finally, once a satisfactory LE design has been achieved, it is verified using Finite Element Limit Analysis (FELA), again with each sections being subjected to a stability analysis.

The automated system requires a computational time of a few hours for a complete pipeline route and thus offers very significant savings and provides the opportunity to modify and optimize the pipeline routing iteratively.

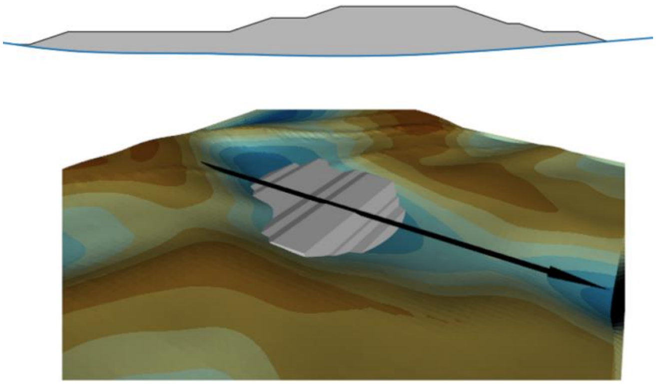

Figure 4: 2D section (top) extracted from 3D geometry (bottom).

2 LIMIT EQUILIBRIUM ANALYSIS

The Limit Equilibrium Method (LEM) is widely used for slope stability analysis (see e.g. Duncan et al. 2006). The basic idea is as follows. First, postulate a failure mechanism given by a slip line. This is typically circular although it in principle is possible to use any shape. The assumed slip line defines the failing mass which is subsequently divided into vertical slices. At the interface defined by the slip line, a normal and shear stress, related to each other by the failure criterion, act. Next, different methods make different assumptions about the inter-slice forces. The two most common assumptions are those of the Ordinary Method of Slices and Bishop's Method. In the former, all inter-slice forces are assumed zero. In the latter, only the inter-slice shear forces are assumed zero.

For the present application, the assumed failure line is as shown in Figure 5. It comprises two straight lines through the rock fill connected by an arc through the seabed. It involves three degrees of freedom as indicated in the figure and is in this way computationally equivalent to a standard circular slip line.

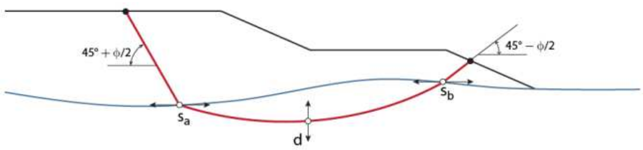

Figure 5. Assumed LE failure mode.

Experience shows that Bishop's method is more accurate for relatively shallow failures while a weighted average of Ordinary and Bishop gives good estimates for deep seated failures. Hence, a weighted method which interpolates between the two former methods, depending on the depth of the failure mechanism, is employed.

3 FINITE ELEMENT LIMIT ANALYSIS

Finite element limit analysis (FELA) is well described in the literature (see e.g. Lyamin & Sloan 2002, Makrodimopoulos & Martin 2006, Krabbenhoft et al. 2007, Sloan 2013) and has by now reached a level of maturity where both 2D and 3D problems are solved on a routine basis (see e.g. Olsen & Krabbenhoft 2021). While classic limit analysis is concerned with the maximum magnitude of a given load that a structure can sustain, the present work is concerned with the complementary problem of determining the Factor of Safety (FOS), i.e. the factor by which the material strengths should be reduced in order to bring the system to a state of incipient collapse. This task may be carried out using repeated feasibility analysis (which is reminiscent of conventional limit analysis) as discussed by Krabbenhoft & Lyamin (2015). For the automated design system described, all design iterations are first carried out using LEM after which they are verified using FELA.

4 LEM VS FELA

In this section, the accuracy of the three different LE methods employed (Ordinary, Bishop and weigthed Ordinary/Bishop) is briefly discussed.

As described in Section 2, the Ordinary Method of Slices tends to underestimate the FOS while Bishop's method tends to provide overestimates. The idea behind the weighted Ordinary/Bishop method is to arrive an optimal compromise between the two.

To verify these assertions, results from a four different berms, comprising in total 96 sections have been analysed. The failure mechansims, examples of which are shown in Figure 6, vary widely between the different sections. The FELA runs were conducted with a large number of elements such that the FOS obtained are practically exact. The correlation between these and the various LE FOS (in the following denoted FOS_{LE}) are as follows (see also Figure 6):

Ordinary: $FOS = 1.09 \cdot FOS_{LE}$
Weigthed: $FOS = 0.97 \cdot FOS_{LE}$
Bishop: $FOS = 0.90 \cdot FOS_{LE}$

Similarly, using a general purpose limit equilibrium package (SLOPE/W), Olsen et al. (2023) have found $FOS = 0.85 \cdot FOS_{LE}$. On the basis of these results we see that Bishop on average is uncoservative, Ordinary is conservative and the weighted scheme is slightly unconservative, though superior to the former two.

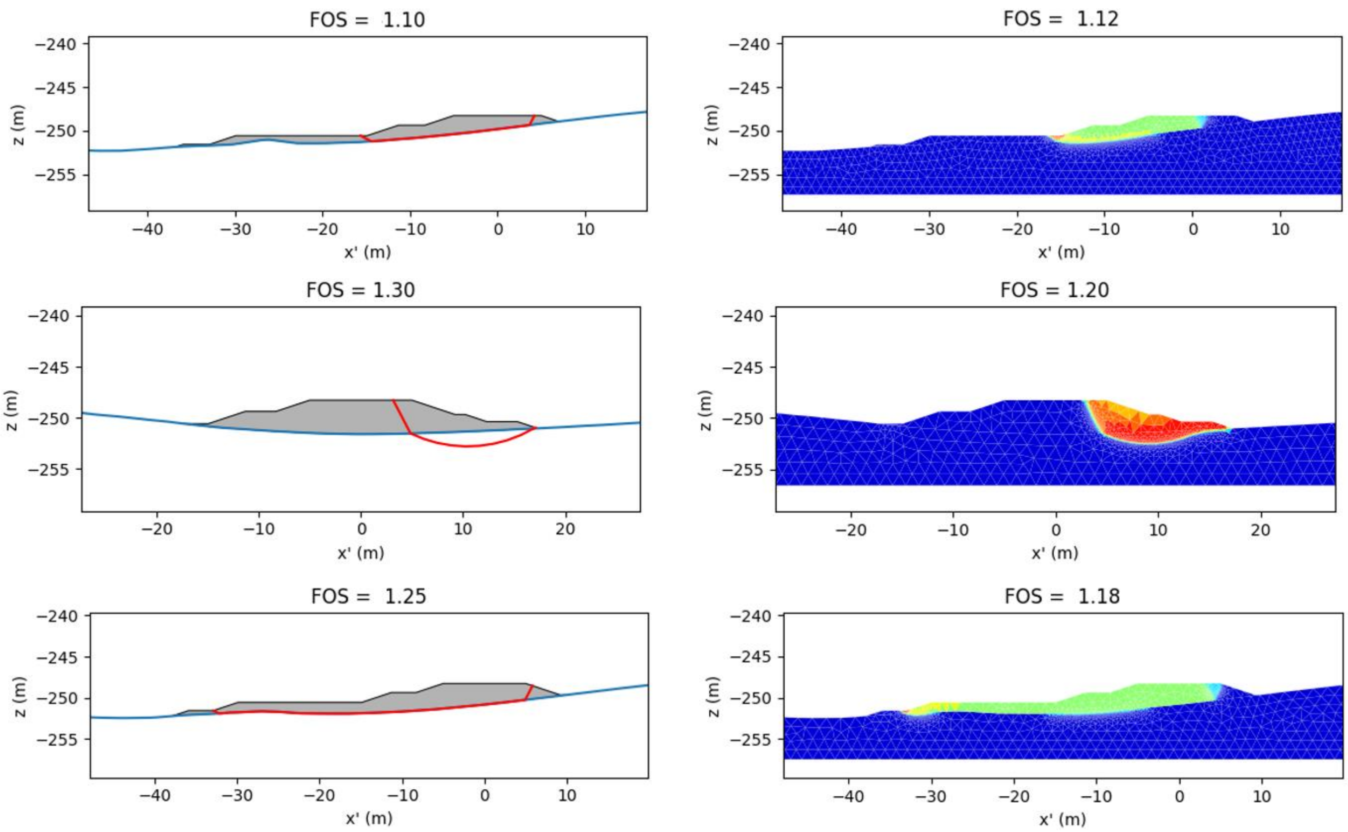

Figure 6. Examples of failure modes: LEM-Weighted (left) and FELA (right).

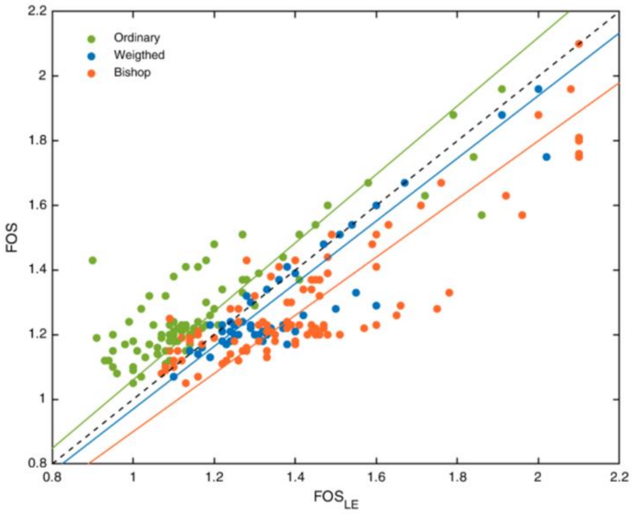

Figure 7: Correlation between FELA FOS and different LEM FOS.

5 EXAMPLE

In the following, we consider the berm shown in Figure 8. The berm is 50 m long and has a volume of 4,152 m^3. The seabed is a very soft clay with an undrained shear strength that increases linearly by 1.64 kPa/m from 1.26 kPa at the top surface. All results are obtained with a plugin that has been developed for the general purpose geotechnical FE program OPTUM GX.

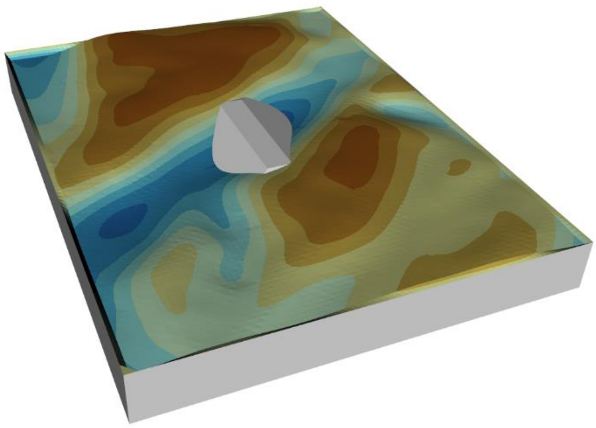

Figure 8: Main berm.

LE-weighted stability analyses for sections along the berm gives the results shown in Figure 9 (negative values here indicate failure on the left while positive values indicate failure on the right).

We see that all FOS are less than 1. The critical (smallest) FOS occurs at s = 18 m. At this location, the failure is as shown in Figure 10.

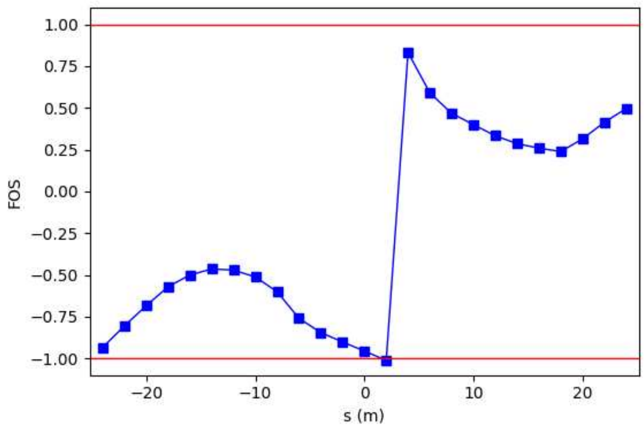

Figure 9: FOS versus distance along the berm (s, with s = 0 corresponding to the centre of the berm).

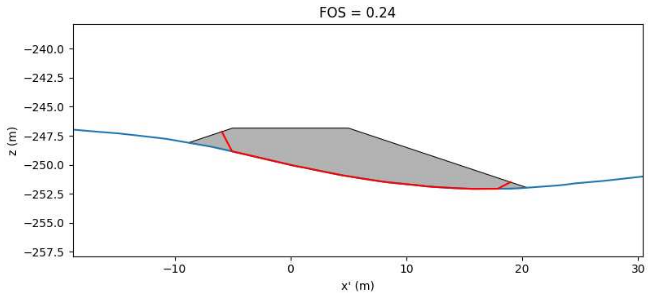

Figure10: Failure mode at s = 18 m.

This failure mode suggests the necessity of counterfill on the right on the berm. Adding such counterfill, and adjusting its length and height iteratively, eventually leads to the situation shown in Figure 11.

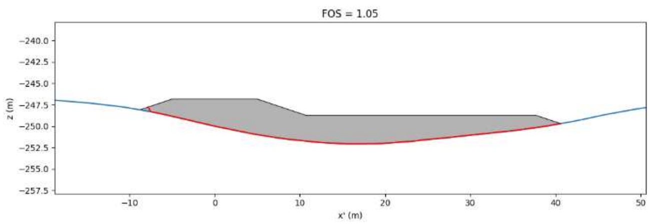

Figure 11: Failure mode at s = 18 m with counterfill added.

Rerunning all sections now provides the results shown in Figure 12.

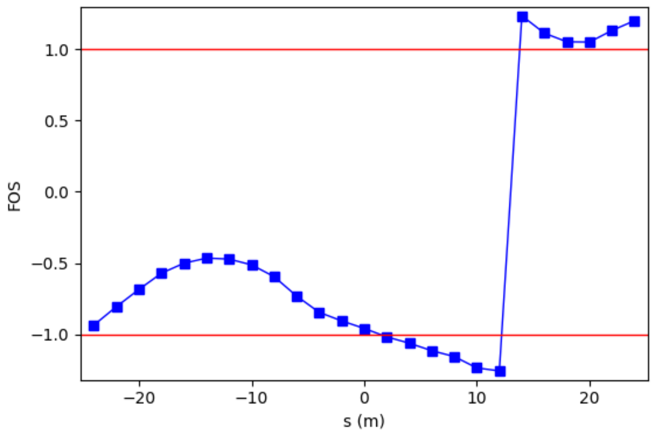

Figure 12: FOS versus distance along the berm.

The critical failure now occurs on the left at s = -14 m as shown in Figure 13. Note that the FOS is negative indicating failure on the left of the main berm.

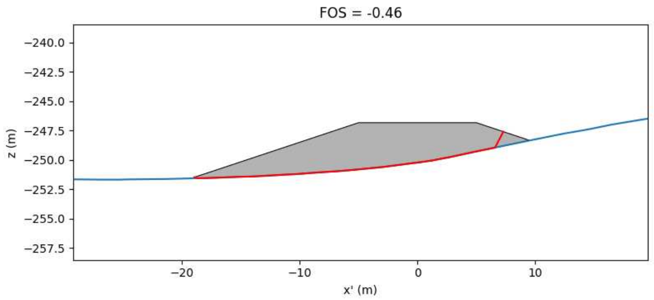

Figure 13: Failure mode at s = -14 m.

Again counterfill is added to bring about the situation shown in Figure 14.

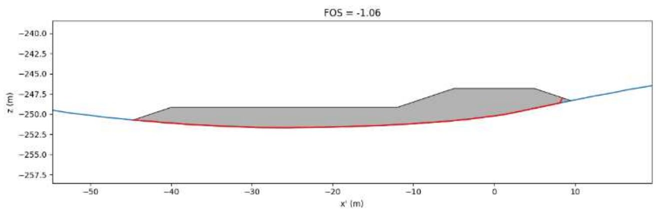

Figure 14: Failure mode at s = -14 m with counterfill added.

Rerunning all sections gives the results shown in Figure 15.

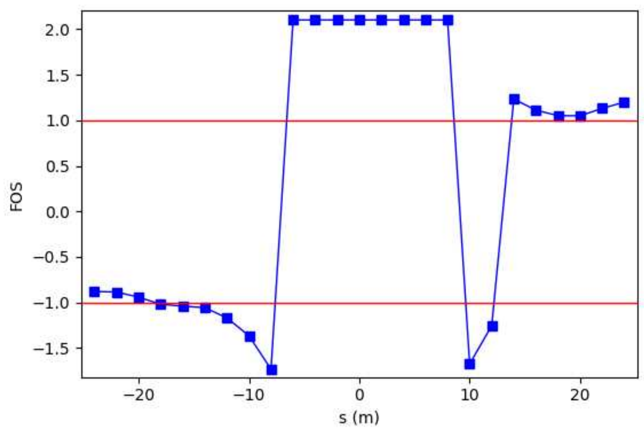

Figure 15: FOS versus distance along the berm.

The critical section is now located at s = - 24 m with the failure mode shown in Figure 16.

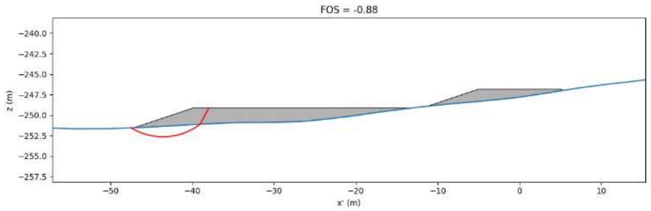

Figure 16: Failure mode at s = -24 m.

The bearing type failure that occurs here can be countered with additional counterfill. However, while the failure shown in Figure 16 in this way is countered, a new one with FOS < 1 occures in the upper part of the berm as shown in Figure 17.

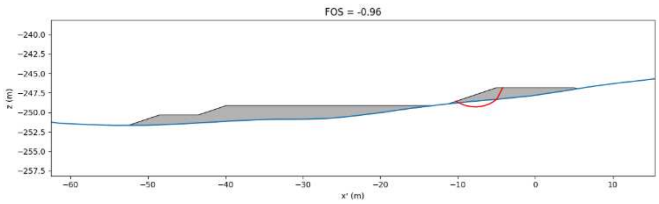

Figure 17: Failure mode at s = -24 m with counterfill added.

This situation is again countered by adding counterfill, now in a way such that the part of the berm at which the failure occurs effectively is strenghtened. This will lead to failure in another section which again is countered, and so on until all sections are stable. At this stage, after 7 iterations, the situation at s = -24 m (which is the critical section) is as shown in Figure 18.

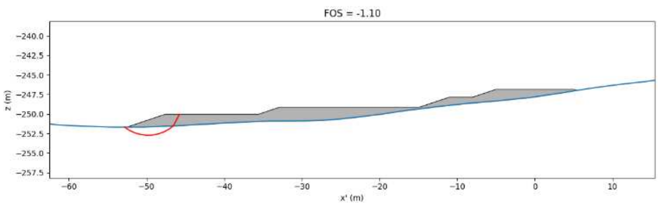

Figure 18: Failure mode at s = -24 m for final design.

At this final stage, the total volume of rock is 7,287 m^3, a 76% increase from the volume of the main berm. The final design is shown in Figure 20.

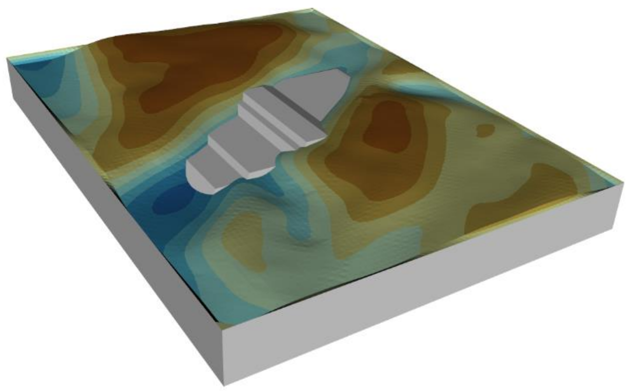

Figure 20: Final design.

The total time for the automated design of the present berm, including FELA verification is about 10 min.

6 CONCLUSIONS

A system for automated design of offshore rock berms has been described. An obvious extension is to include a 3D FELA verification, i.e. to operate on the actual geometry rather than selected 2D sections. This work is ongoing.

7 REFERENCES

Duncan, M.J., Wright, S.G. & Brandon, T.L. 2006. Soil Strength and Slope Stability, Wiley.

Eiksund, G., Brennodden, H., Paulsen, G. & Witsø, S.A. 2008. Ormen Lange Pipelines – Geotechnical challenges, *Proc. Eighteenth International Offshore and Polar Engineering Conference*, Vancouver, Canada, July 2008. Paper Number: ISOPE-I-08-332

Krabbenhoft, K., Lyamin, A.V. & Sloan, S.W. 2007. Formulation and solution of some plasticity problems as conic programs, *International Journal of Solids and Structures,* 44(5), 1533-1549.

Krabbenhoft, K. & Lyamin, A.V. 2015. Strength reduction finite-element limit analysis, *Geotechnique Letters,* 5(4), 250-253.

Lyamin, A.V. & Sloan, S.W. 2006. Lower bound limit analysis using non-linear programming, *International Journal for Numerical Methods in Engineering,* 55(5), 573-611.

Makrodimopoulos, A. & Martin, C.M. 2006. Lower bound limit analysis of cohesive-frictional materials using second-order cone programming, *International Journal for Numerical Methods in Engineering,* 66(4), 604-634.

Olsen, C. & Krabbenhoft, K. 2021. Case study on advanced 3D finite element limit analysis of counter-acts installed at Ormen Lange, *IOP Conf. Ser.: Mater. Sci. Eng.,* 1201 012009.

Olsen, C., Lodahl, M.R. & Kristoffersen, A. 2023. Advanced rock berm design in iceberg plough marks for pipeline support, *OSIG Conf.* (to be presented).

Sloan, S.W. 2013. Geotechnical stability analysis, *Geotechnique,* 63(7), 531-571.